Title

UVB radiation generates sunburn pain and affects skin by activating epidermal TRPV4 ion channels and triggering endothelin-1 signaling

Journal

Proceedings of the National Academy of Sciences of the United States of America, 110(34)

ISSN

0027-8424

Authors

Moore, Carlene
Cevikbas, Ferda
Pasolli, H Amalia
et al.

Publication Date

2013-08-20

DOI

10.1073/pnas.1312933110

Peer reviewed

UVB radiation generates sunburn pain and affects skin by activating epidermal TRPV4 ion channels and triggering endothelin-1 signaling

Carlene Moore[a], Ferda Cevikbas[b,1], H. Amalia Pasolli[c,1], Yong Chen[a,2], Wei Kong[e,2], Cordula Kempkes[b,2], Puja Parekh[a], Suk Hee Lee[a], Nelly-Ange Kontchou[a], Iwei Yeh[b], Nan Marie Jokerst[e], Elaine Fuchs[c,d,3], Martin Steinhoff[b,3], and Wolfgang B. Liedtke[a,f,3]

[a]Liedtke Laboratory, Departments of Neurology and Neurobiology, and [e]Jokerst Laboratory, Department of Electrical Engineering, Duke University, Durham, NC 27710; [b]Steinhoff Laboratory, Departments of Dermatology and Surgery, University of California, San Francisco, CA 94115; [c]Fuchs Laboratory of Mammalian Cell Biology and Development and [d]Howard Hughes Medical Institute, The Rockefeller University, New York, NY 10021; and [f]Clinics for Pain and Palliative Care, Duke University Medical Center, Durham, NC 27705

Contributed by Elaine Fuchs, July 10, 2013 (sent for review June 7, 2013)

At our body surface, the epidermis absorbs UV radiation. UV overexposure leads to sunburn with tissue injury and pain. To understand how, we focus on TRPV4, a nonselective cation channel highly expressed in epithelial skin cells and known to function in sensory transduction, a property shared with other transient receptor potential channels. We show that following UVB exposure mice with induced *Trpv4* deletions, specifically in keratinocytes, are less sensitive to noxious thermal and mechanical stimuli than control animals. Exploring the mechanism, we find that epidermal TRPV4 orchestrates UVB-evoked skin tissue damage and increased expression of the proalgesic/algogenic mediator endothelin-1. In culture, UVB causes a direct, TRPV4-dependent Ca^{2+} response in keratinocytes. In mice, topical treatment with a TRPV4-selective inhibitor decreases UVB-evoked pain behavior, epidermal tissue damage, and endothelin-1 expression. In humans, sunburn enhances epidermal expression of TRPV4 and endothelin-1, underscoring the potential of keratinocyte-derived TRPV4 as a therapeutic target for UVB-induced sunburn, in particular pain.

calcium-permeable channels | epithelial–neuronal cross-talk | photodermatitis | phototransduction

The surface epithelium (epidermis) of skin provides barrier protection against dehydration and the potentially harmful external environment (1). Accordingly, skin is the site of first interaction between ambient environment and immunologically competent organismal structures, and also the site for sentient responses (2). Sensory neurons in the dorsal root ganglia (DRG) and trigeminal ganglia (TG) are endowed with sensory transduction capacity for heat, cold, mechanical cues, itch, and pain, and their axons directly interface with skin epithelium (2–4).

Against a background of suggestive findings (2, 5–7), we wondered whether the epidermis as a "forefront" of sensory signaling may function in sensitizing pain transduction in response to naturally occurring irritating cues. To elucidate mechanisms, we used a mouse sunburn model and induced a state of lowered sensory thresholds associated with tissue injury caused by UV radiation (8–10). UV-sunburn-evoked lowering of sensory thresholds shares major hallmarks of pathological pain, a valuable feature of this model. Skin tissue injury caused by UVB has been elucidated to be mediated by cytokines and chemokines, known from immunological responses, such as IL-1β and IL-6, which are also known to cause and facilitate pain (11–19). Another more recent study identified a proinflammatory chemokine, CXCL5, as proalgesic in response to UVB overexposure of rat and human skin (20). An exciting new arena pertaining to molecular mechanisms of the skin's response to noxious UV was recently opened by an elegant study that reported the role of UVB-mediated damage to noncoding RNA molecules in the skin (21). Unraveling a molecular mechanism, the *Toll-like receptor 3* gene was found critical in signaling the proinflammatory actions of the UVB-damaged noncoding RNA molecules. However, this study focused on molecular mechanisms of acute inflammation in the skin.

We intended to identify pain mechanisms that mediate the pain associated with UVB-mediated tissue injury. Pain in response to external environmental cues has been understood better because of scientific progress in the field of transient receptor potential (TRP) ion channels that have been found responsive to such cues, and which were found expressed in DRG and TG peripheral sensory neurons, which are the cells believed to be the primary transducers. Indeed, TRPV1, one of the founding members of the TRPV channel subfamily, has been identified as relevant for pain, including pathological pain, response to thermal cues, and most recently for itch (22–31). However, TRPA1 (transient receptor potential ion channel, ankyrin subfamily, family member #1) and TRPM8 seem to be involved in transduction of pain-inducing stimuli as well (32–36).

Also a family member of the TRPV subfamily, TRPV4 is a multimodally activated, nonselective cation channel that is involved in physiological pain evoked by osmotic and mechanical, but not thermal, cues (37–40). For pathological pain, it is relevant for inflammation- and nerve-damage-induced pain sensitization (41–43). Of note, $Trpv4^{-/-}$ mice exhibit impaired skin-

Significance

Skin protects against harmful external cues, one of them UV radiation, which, upon overexposure, causes sunburn as part of the UVB response. Using genetically engineered mice and cultured skin epithelial cells, we have identified the calcium-permeable TRPV4 ion channel in skin epithelial cells as critical for translating the UVB stimulus into intracellular signals and also into signals from epithelial skin cell to sensory nerve cell that innervates the skin, causing pain. These signaling mechanisms underlie sunburn and in particular sunburn-associated pain. Thus, activation of TRPV4 in skin by UVB evokes sunburn pain, highlighting the forefront-signaling role of the skin and TRPV4.

Author contributions: C.M., N.M.J., E.F., M.S., and W.B.L. designed research; C.M., F.C., H.A.P., Y.C., W.K., C.K., P.P., S.H.L., N.-A.K., I.Y., and W.B.L. performed research; W.K., N.M.J., and M.S. contributed new reagents/analytic tools; C.M., F.C., H.A.P., E.F., M.S., and W.B.L. analyzed data; and E.F., M.S., and W.B.L. wrote the paper.

The authors declare no conflict of interest.

Freely available online through the PNAS open access option.

[1]F.C. and H.A.P. contributed equally to this work.

[2]Y.C., W.K., and C.K. contributed equally to this work.

[3]To whom correspondence may be addressed. E-mail: fuchslb@rockefeller.edu, steinhoffm@derm.ucsf.edu, or wolfgang@neuro.duke.edu.

This article contains supporting information online at www.pnas.org/lookup/suppl/doi:10.1073/pnas.1312933110/-/DCSupplemental.

barrier function (44, 45). That said, TRPV4 is expressed in a number of different cell types, including robust expression in epidermal keratinocytes and also is detectable in skin-innervating sensory neurons. This "dual-location expression" of TRPV4 leaves the cellular mechanisms involved in the channel's function and the functional contribution of environment-exposed keratinocytes vs. skin-innervating sensory neurons unclear.

Against this background of dual-location TRPV4 expression and the role of TRPV4 in inflammatory and neuropathic pain, we now address whether epidermally derived TRPV4 is pathophysiologically relevant in sunburn pain and tissue damage. Using *Trpv4* gene-targeted mice, selectively inducing targeting in postnatal keratinocytes, and topically applying selective TRPV4 inhibitors, we demonstrate that epidermal TRPV4 plays a prominent, hitherto unrecognized role in UVB-evoked skin tissue damage and pain of sunburn.

Results

Epidermal-Specific, Tamoxifen-Inducible *Trpv4* Null Mouse: Nocifensive Behavior. To circumvent developmental issues that can arise in gene-targeted mice with ubiquitous deletions, we developed an inducible conditional system to assess the roles of TRPV4 in sunburn and pain. Using mouse ES cells, we first built *Trpv4*$^{lox/lox}$ mice that were mated with Keratin-14 (K14)-CRE^{ER} transgenic mice, described previously (46). Additional details are shown in Fig. S1 *A* and *B*.

We focused on adult glandular mouse hind-paw-pad skin for our analyses, because it more closely resembles human skin (47). Tamoxifen induction at 8 wk of age resulted in efficient ablation of *Trpv4* expression in skin epidermis, as judged by anti-TRPV4 immunolabeling, quantitative RT (qRT)-PCR, and Western blotting (Fig. 1*A*). Given the established dependence of skin renewal on keratinocyte Ca^{2+} signaling, it was surprising that *Trpv4* knockdown did not result in gross alterations of skin structure or in induction of the terminal differentiation-specific marker keratin-1 (K1), which is known to be governed by elevated Ca^{2+} influx suprabasally (Fig. 1*A* and Fig. S1*C*). Although basal progenitor marker K14 was aberrantly sustained suprabasally in these mice, overall cyto- and layer architecture of the epidermis (also discussed below in the histopathology analysis) appeared normal, and no obvious visual changes of the skin/epidermis of tamoxifen (tam)-treated inducible *Trpv4* knockout (iKO) mice were detected.

Peripheral sensory neurons innervating the paw pad still showed robust expression of TRPV4 (Fig. S1*D*). This enabled us to evaluate whether epidermal *Trpv4* deficiency critically affects UVB-mediated nocifensive behaviors. For this purpose, we assayed two relevant sensory submodalities, thermal and mechanical, and compared our iKO mice to pan-null *Trpv4*$^{-/-}$ and their WT controls (Fig. 1*B*). Forty-eight hours after UV exposure, both tam-treated iKO and *Trpv4*$^{-/-}$ mice displayed significantly reduced sensitivity to noxious radiant heat (Hargreaves' test), and also toward noxious mechanical stimulation (automated von Frey hair testing), compared with their respective controls. Thus, surprisingly, epidermal-specific TRPV4 deficiency seemed to be equivalent to *Trpv4* pan-null in reducing UVB-induced behavioral sensitization, namely in attenuating thermal and mechanical allodynia.

Further underscoring the importance of epidermal TRPV4 in regulating nocifensive behavior, a correlation existed between UV-induced sensitization to thermal stimuli and the level of *Trpv4* gene knockdown, particularly at <0.45 times the WT levels of *Trpv4* mRNA (Fig. 1*C*). This indicates the presence of a threshold for *Trpv4* knockdown to influence nocifensive behavior.

For comparison with a well-established pain model in which the injurious stimulus has sufficient involvement with both epidermis and skin-innervating sensory neurons, we used the formalin model and induced irritation with paw-pad injections of formalin, eliciting the established biphasic nocifensive response, which manifests within 1 h (48). In this assay, conditional epidermal knockdown of TRPV4 had no effect on direct peripheral chemical irritation (phase I) or the early maladaptive neural response (phase II) (Fig. 1*D*). Taken together, the level of epidermal *Trpv4* knockdown was the determining factor for the degree of attenuation of nocifensive behavior caused by UVB irradiation. We notice a selectivity for sunburn pain because chemical irritant-induced nocifensive behavior was not affected.

In additional experiments, we attempted to verify eventual TRPV4 expression in epidermal Merkel cells because they play a role in tactile discrimination and light touch (49, 50), which becomes allodynic in sunburn. We could not detect TRPV4 protein in Merkel cells (Fig. S1*E*), possibly indicating low-level expression because *Trpv4* mRNA has been detected in these cells (51, 52). Detectable TRPV4 would have allowed us to address whether there is a reduction of expression by inducible K14-CRE, given that a portion of Merkel cells (~25%) has been found to express K14 (53, 54). In view of these considerations, we cannot exclude a possible ancillary role of TRPV4 channel expression in skin Merkel cells in the pathogenesis of pain, in particular touch allodynia, in sunburn.

Additional controls showed us that *Trpv4*$^{lox/+}$ heterozygous mice had virtually identical behavioral sensitization (similar to WT) in response to UVB, irrespective of CRE induction with tam or vehicle (Fig. S1*F*). These findings exclude a functional role for CRE^{ER} on its own and reiterate the specificity of our approach in targeting *Trpv4* ablation to keratinocytes.

Activation Markers of Skin-Innervating Peripheral Neurons Support Behavioral Findings. In WT mice, the paw pad is innervated by L5 DRG sensory neurons. Significant subpopulations of DRG and TG sensory neurons express TRPV4, allowing us to examine whether there are changes in their TRPV4 expression in response to induction of K14 (46). TRPV4 expression was unchanged with paw-pad exposure to UVB, an external cue known to sensitize innervating neurons (10) (Fig. S1*D*). Interestingly, whereas sensitization could be verified in control mice, it was absent in tam-treated iKO mice, as documented by labeling for phosphorylated ERK (pERK), a known marker of sensory neuron activation in response to inflammation and irritation (43, 55) (Fig. 1*E*). Furthermore, size measurements of pERK-expressing L5 DRG neurons revealed them to be small to medium-size (<30 μm in diameter), suggesting their possible involvement in relay of noxious stimuli (Fig. S1*G*). These results underscore a role for epithelial-expressed TRPV4 in governing UVB-induced activation of skin-innervating DRG sensory neurons in sunburn pain.

UVB-Induced Tissue Damage Depends upon Epidermal Expression of TRPV4. To understand how loss of TRPV4 affects UVB-induced tissue damage, we performed light microscopy and ultrastructural analyses (Fig. 2 *A* and *B* and Fig. S2 *A*–*C*). In response to UVB, robust signs of sunburn tissue damage appeared in control skin, as evidenced by intraepidermal infiltrates of granulocytes and focal blistering. In skin of tam-treated iKO mice with incomplete targeting, damage was present, perhaps moderately less severe. In striking contrast, however, in skin of tam-treated iKO mice with complete targeting, no signs of tissue injury were seen. These data demonstrate convincingly that epidermal TRPV4 is necessary for skin to show a tissue-injury response to UVB with epidermal structural changes and reactive cell recruitment, and tissue injury is attenuated when epidermal TRPV4 is knocked down.

We next extended our characterization of TRPV4-dependent epidermal injury by using suitable immuno-histopathology markers for the different cell types involved. We used IL-6 as a marker of activated keratinocytes. In addition, IL-6 is inherently algogenic (14). IL-6 immunoreactivity was robustly up-regulated in

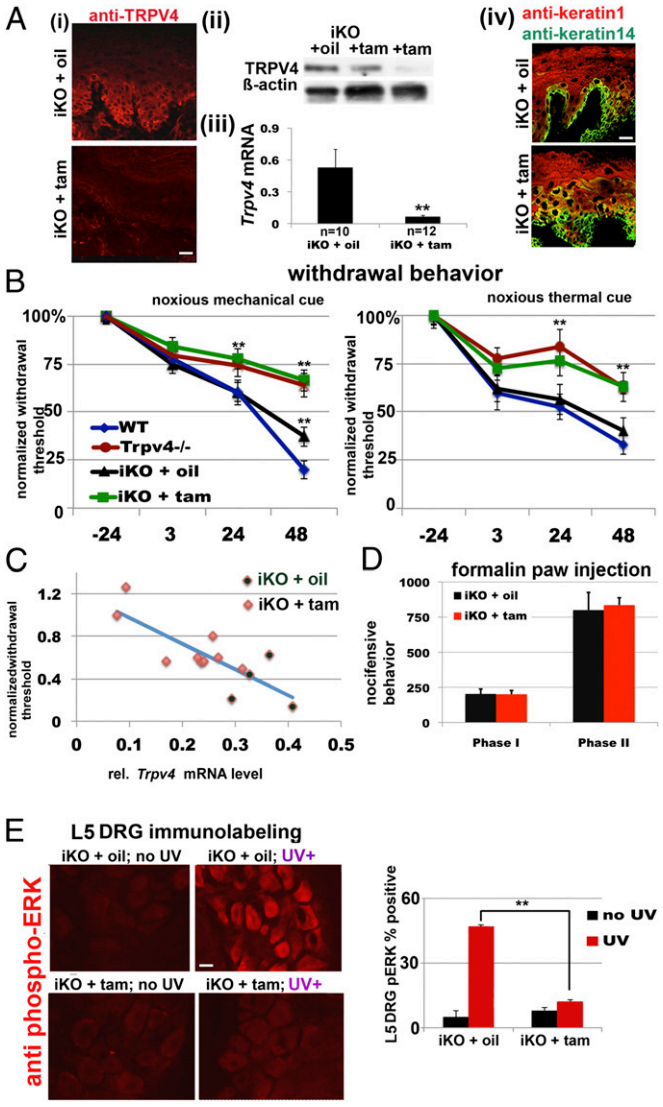

Fig. 1. Keratinocyte-specific ablation of *Trpv4* leads to alterations in nocifensive behavior in response to UVB. (*A*) Epidermal TRPV4 expression and its loss upon keratinocyte-specific ablation of *Trpv4* in tam-induced iKO mice. (*i*) TRPV4 immunofluorescence. Note TRPV4 in epidermis of vehicle (oil)-treated control, but not tam-induced iKO mice. (Scale bar, 10 μm.) (*ii*) Western blot of epidermal lysates from paw-pad skin. Note knockdown and more complete loss of TRPV4 following induced *Trpv4*-ablation (β-actin used for normalization). (*iii*) qRT-PCR for *Trpv4* mRNA from paw-pad skin is shown, indicating significant *Trpv4* knockdown in response to tam treatment vs. carrier (oil). $P < 0.0001$, *t* test. (*iv*) Immunofluorescence for epidermal lineage markers. In WT skin, basal epidermal marker K14 is downregulated and suprabasal marker K1 is induced upon commitment to terminal differentiation. Upon knockdown of TRPV4, this balance seems perturbed, with some spinous layer cells showing colabeling. (Scale bar, 10 μm.) (*B*) Nocifensive behavior in response to UVB exposure. Time course (in hours) for nocifensive behavior elicited by either a noxious mechanical stimulus (automatic von Frey hair assay, *Left*) or thermally evoked nocifensive behavior (Hargreaves' assay, *Right*). Note significantly less sensitization in $Trpv4^{-/-}$ and in tam-treated iKO mice, relative to oil-treated (vehicle) iKO and WT mice. $n \geq 10$ animals per group; $^{**}P < 0.01$ ANOVA. (*C*) Correlation between nocifensive behavior and level of *Trpv4* knockdown; $n = 12$ animals are shown for which both parameters were available and *Trpv4* mRNA levels <0.45. Note the four vehicle-induced animals (green symbols) vs. their tam-induced counterparts (red symbols). (*D*) Loss of epidermal TRPV4 shows no significant effect on nocifensive behaviors caused by formalin injection. Bars depict average cumulative nocifensive behavior within the first 10 min (phase I), and 10–45 min (phase II) postinjection; $n = 4$ per group. (*E*) pERK in L5 DRG neurons. pERK immunofluorescence of L5 DRG sections are shown for oil- and tam-treated iKO animals ± exposure to UVB. Note that only UVB-exposed control mice show pERK expression in the paw-pad-innervating L5 DRG. Quantifications are shown at right; $n = 3$ animals per group, six sections per DRG per animal, $^{**}P < 0.01$ ANOVA.

UVB-exposed epidermis of control mice and, in contrast, virtually eliminated in iKO and pan-null $Trpv4^{-/-}$ skin (Fig. 3*A* and Fig. S2*D*). Because it reflects epidermal activation by UVB and is also causing pain, we assessed *Il-6* gene expression by determining its mRNA abundance with qRT-PCR. We compared $Trpv4^{-/-}$ with WT skin at time points 2 h and 24 h. In WT epidermis we found a significant early up-regulation at time point 120 min, sustained at 24 h. In contrast, the absence of *Trpv4*, *Il-6* mRNA was not regulated. These findings suggest early activation of the skin epithelium by UVB and its maintenance by ongoing tissue injury.

Both macrophages and neutrophils are known to contribute to pain via proalgesic/algogenic mediators (56). As evidenced by immunostaining for CD68 (macrophages) and neutrophil-specific elastase [known to enhance nociception (57)], UVB-induced tissue infiltration of both cell types was markedly reduced in the skin of iKO mice (Fig. 3 *B* and *C*). In contrast, mast cell abundance was not different (Fig. S2*E*). Taken together, these findings show that keratinocytes' TRPV4 expression is critical for their UVB-mediated activation. Epithelial activation attracts macrophages and pain-enhancing neutrophils in response to UVB.

TRPV4 Sustains the UVB-Induced Ca^{2+} Response in Primary Mouse Keratinocytes. To image Ca^{2+} dynamics of primary mouse epidermal keratinocytes (1°MK) following UVB exposure, we built a customized device that enabled us to apply specific and narrowband UVB stimulation in vitro (Fig. 4 *A* and *B* and Fig. S3 *A–D*). The elicited Ca^{2+} signal was diminished by a UV-refracting glass coverslip, underscoring the dependence of the Ca^{2+} response on UVB (Fig. 4*C* and Fig. S3*A*).

Next, we asked whether the UVB-mediated Ca^{2+} response is dependent on extracellular Ca^{2+} and recorded affirmative findings by sequential exposure to UVB-extracellular Ca^{2+} (Fig. 4*D*). This finding prompted us to directly query the role of TRPV4 in the UVB-mediated Ca^{2+} response. Indeed, 1°MK from $Trpv4^{-/-}$ mice exhibited a greatly diminished response relative to their WT counterparts (Fig. 4*E*). Moreover, when a selective TRPV4 blocker, GSK205 (43, 58, 59), was used, WT 1°MK showed responses similar to those of $Trpv4^{-/-}$ 1°MK (Fig. 4*F*).

In view of the known TRPV3 expression in keratinocytes (60, 61), we also addressed TRPV3's role in UVB-mediated Ca^{2+} increase but observed no effect with the TRPV3-selective inhibitor isopentenyl pyrophosphate (IPP) (Fig. 4*G*). The same dose of IPP was effective in inhibiting camphor-evoked Ca^{2+} transients (Fig. S3*E*).

Together, our experiments indicate that epidermal UVB exposure elicits the influx of extracellular Ca^{2+} through TRPV4, and not TRPV3, channels. Because both channels are present, our data further suggest that TRPV4 channels are selectively activated by UVB light. We obtained corroborating findings by chemically activating TRPV4 with GSK101, which directly stimulated TRPV4 in WT 1°MK. The GSK101-mediated response was dependent upon external Ca^{2+} and was eliminated by the TRPV4 inhibitor GSK205 (Fig. S3*F*), similar to UVB-evoked Ca^{2+} dynamics.

To assess whether TRPV4 is sufficient for the UVB-evoked Ca^{2+} influx, we ectopically expressed TRPV4 in HEK293 epithelial cells. Directed TRPV4 expression resulted in appreciable Ca^{2+} signaling in response to UVB (Fig. S3*G*), which could be blocked by GSK205. Thus, heterologous TRPV4 expression is sufficient for UVB radiation to cause Ca^{2+} transients.

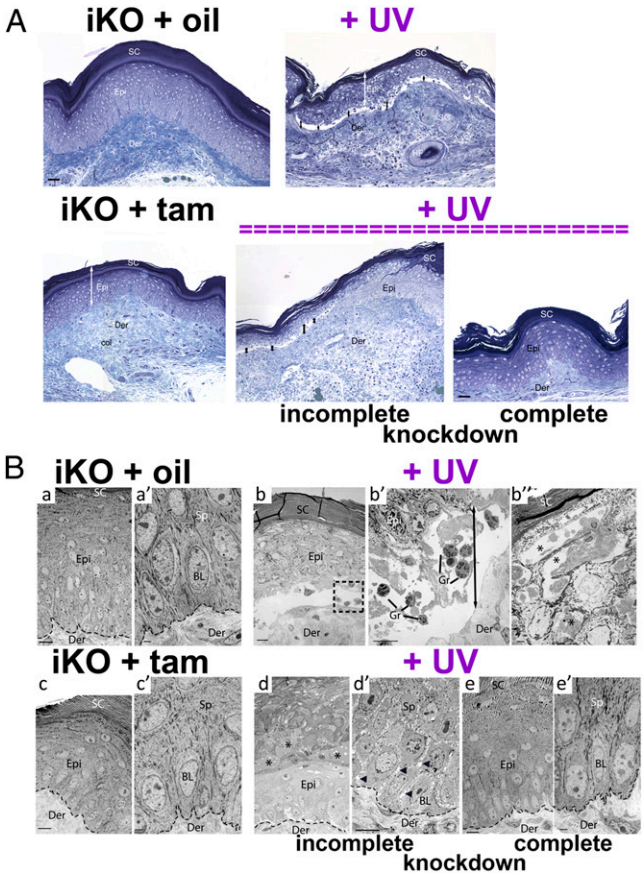

Fig. 2. Structural and ultrastructural analyses showing that UVB-mediated skin tissue injury depends upon keratinocyte TRPV4. (*A*) Toluidine blue semithin (1-μm) sections. Micrographs show representative findings of skin in response to UVB, sampled 48 h after UVB exposure. Note that upon UVB stimulation oil- (TRPV+), but not tam-treated (TRPV−), iKO mice exhibit separations at the epidermal–dermal boundary and robust signs of tissue injury including influx of neutrophil granulocytes. Note also that just beneath the stratum corneum (SC) the upper epidermis shows extensive structural damage, which could also be seen in skin of tam-treated iKO mice in which *Trpv4* knockdown was incomplete, but not in those animals in which it was more complete (Fig. S2*A*). (Scale bars, 20 μm.) Der, dermis; Epi, epidermis. (*B*) Ultrastructural findings by EM. Selected areas from 1-μm semithin sections of paw skin were examined by transmission electron microscopy. *a* and *a*′ and *c* and *c*′ show normal epidermal (Epi) structure for both oil- and tam-treated iKO mice, in the absence of UVB stimulation. *a* and *c* show an intact epidermis. Basal (BL) and spinous (Sp) layers are magnified *a*′ and *c*′ displaying a normal organization with no evidence of epidermal damage. *b*, *b*′, *b*″, *d*, *d*′, and *e*, *e*′ show representative findings of skin in response to UVB, sampled 48 h after UVB exposure. (*b*) Disrupted epidermis in oil-treated iKO mice. An area equivalent to the boxed area is magnified in *b*′, where granulocyte infiltration of epidermis is evident (Gr) and blistering with detachment of the epidermis from the dermis (double arrows). (*b*″) Upper part of epidermis in contact with SC, showing extensive vacuolization and deposits of fibrin inside the vacuoles (asterisks). (*d*) Tamoxifen-treated iKO mice with incomplete knockdown of *Trvp4* show skin phenotype similar to oil-treated iKO mice, with robust signs of tissue damage to basal and spinous layer, fibrin deposits (asterisks), and intercellular spaces (arrowheads in *d*′). (*e*) Intact epidermis in iKO with complete knockdown of *Trvp4,* with normal basal and spinous layers in *e*′. Dotted lines indicate the dermal–epidermal boundary. (Scale bars, 20 μm for *a*, *b*, *c* and *d*; 10 μm for *b*′ and *e*′, and 2 μm for the other micrographs.)

Endothelin-1 Is a Critical Epidermal Effector of the UVB–TRPV4–Ca^{2+} Response. The UVB–TRPV4–Ca^{2+} response depended on phospholipase C (PLC), because it was virtually eliminated by the specific PLC inhibitor U73122 (Fig. 4*H*), suggesting that lipid products of PLC [e.g., inositol trisphosphate (IP3)] might be involved. It also hinted at possible involvement of G protein-coupled receptor signaling.

Using a candidate approach, we focused on endothelin receptors [ET(R)s], which are known to be expressed in skin keratinocytes (62). ET(R)s were suitable candidates because they are known to function in pain signaling (63) and because their cognate peptide ligand, endothelin-1 (ET1), is elevated when keratinocytes are exposed to UVB (64). When 1°MK were exposed to ET1, they exhibited a significant increase in UVB-induced Ca^{2+} signaling (Fig. 5 *A*, *i*). This response was dependent on TRPV4, because it was greatly diminished by GSK205. Consistent with this result, ET1 augmented chemical TRPV4 activation with GSK101 (Fig. S4*A*).

We next blocked ET1 secretion by applying the proendothelin convertase inhibitor CGS35066. This inhibitor significantly diminished UVB-induced Ca^{2+} signaling in 1°MK (Fig. 5 *A*, *i*). Could autocrine/paracrine ET1 signaling to its cognate ET(R)s underlie the observed Ca^{2+} signal, which depended on TRPV4? In agreement, ET(R) inhibitors attenuated the Ca^{2+} signal in response to UVB/ET1 coexposure. Interestingly, antagonism of ET-R(A), using BQ123, eliminated later phases of the Ca^{2+} response, while leaving the initial rise unaffected; by contrast, ET-R(B) antagonism, using BQ788, converted the UVB–Ca^{2+} response into a more protracted one (Fig. 5 *A*, *ii*). Coapplication

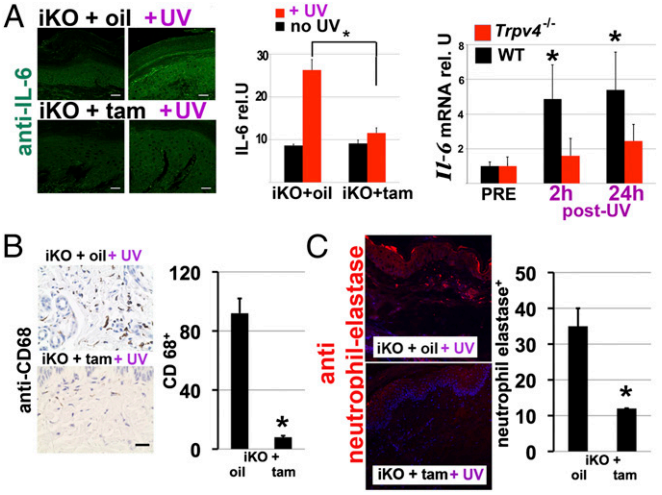

Fig. 3. Immuno-histochemical analysis demonstrates that UVB-mediated activation of keratinocytes and recruitment of macrophages and neutrophils depends upon keratinocyte TRPV4. (*A*) IL-6 up-regulation in keratinocytes as a marker of epidermal activation. IL-6 immunofluorescence reveals a reduced ability of TRPV4-deficient mice to elevate keratinocyte IL-6 expression in response to UVB exposure. Quantifications for protein are shown next to micrograph. Densitometries are for $n \geq 3$ mice per group, showing significant up-regulation for oil-treated iKO mice, and lack thereof for tam-treated mice. (*Right*) Bar diagram shows *Il-6* mRNA quantification and time course. *Il-6* mRNA was determined by qPCR after isolation of total RNA from paw-pad epidermis. Note the early and robust increase, albeit with variation, at the 2-h time point, in WT control epidermis, in contrast to the very moderate increase in $Trpv4^{-/-}$ epidermis. Note also the sustained robust up-regulation at 24 h, again moderately up-regulated in $Trpv4^{-/-}$ epidermis. Quantifications are for n = 8–12 mice per group. *Statistically significant (P = 0.011, *t* test). (Scale bar, 20 μm.) (*B*) Recruitment of macrophages in UVB-exposed skin. Note that the numbers of dermal CD68+ macrophages induced by UVB exposure in control mice is significantly reduced when *Trpv4* is ablated in the epidermis. Quantifications are shown at right (n = 3 mice per group; *$P < 0.05$ *t* test). (Scale bar, 20 μm.) (*C*) Recruitment of elastase-expressing neutrophils to UVB-exposed skin. Shown are representative immunofluorescence micrographs and respective quantifications. Note a strong increase in abundance of elastase-expressing neutrophils in control mice, and a lack thereof in tam-treated iKO mice. n = 4 mice per group, *$P < 0.05$ *t* test. (Scale bar, 40 μm.)

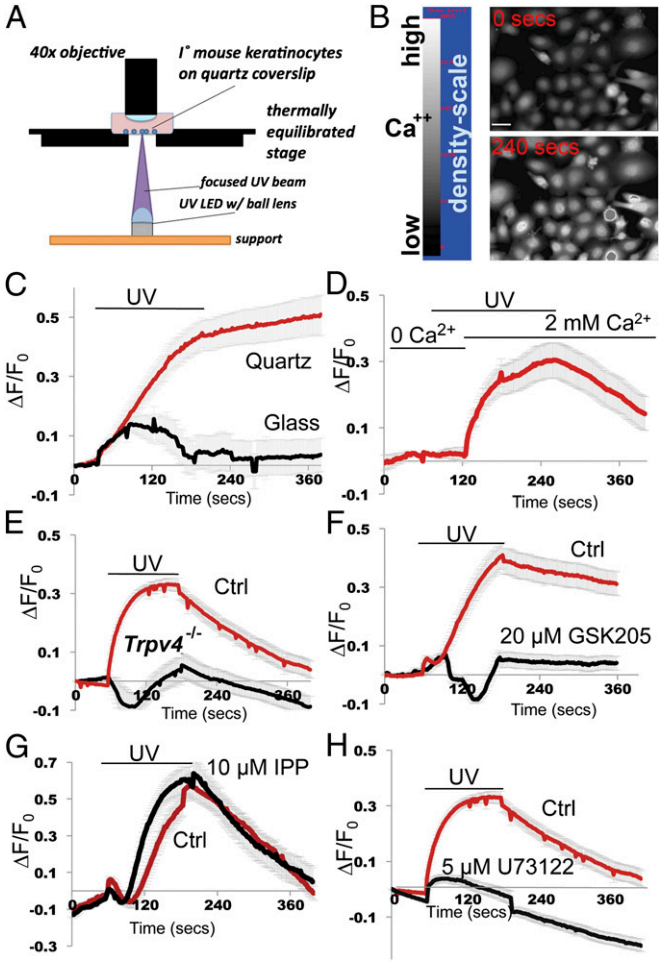

Fig. 4. Ca^{2+} influx into keratinocytes in response to UVB depends on TRPV4. (*A*) Custom-built UVB cell illumination apparatus (see also Fig. S3). (*B*) Fluo-4 Ca^{2+} imaging in 1°MKs. Fluorescent micrographs of 1°MKs after loading with Ca^{2+}-sensitive dye, fluo-4, before (*Upper*) and at the end of UVB exposure (*Lower*). (Scale bar, 10 μm.) (*C–H*) UVB-evoked Ca^{2+} dynamics. Fluo-4 imaging was used to detect Ca^{2+} transients in 1°MKs following UVB exposure. *y* axis indicates the increase in fluorescence, ΔF, normalized for prestimulation signal, F_0 ($\Delta F/F_0$). The signal shown is that averaged from ≥50 cells. (*C*) Ca^{2+} signaling is dependent upon UVB, and is strikingly reduced when quartz coverslips are replaced by glass coverslips. Analysis of UVB permeation for glass vs. quartz indicates that 13.7% of the UVB permeates glass vs. 88.9% for quartz (see also Fig. S3*A*). Given the attenuation of the UVB-evoked signal with glass coverslip, this provides clear indication of a dose–response relationship. Note also that the Ca^{2+} signal with quartz coverslip in WT 1°MKs persisted after UVB, as was sometimes observed. (*D*) UVB-evoked Ca^{2+} signaling is dependent on external [Ca^{2+}]. (*E*) UVB-evoked Ca^{2+} signaling is not seen in $Trpv4^{-/-}$ 1°MKs, revealing the importance of the TRPV4 ion channel. (*F*) UVB-evoked Ca^{2+} signaling is strongly down-regulated in the presence of TRPV4-selective inhibitor, GSK205 (20 μM). (*G*) The UVB-evoked Ca^{2+} signal is not inhibited by the TRPV3-selective inhibitor, IPP. For validation of IPP's activity, see Fig. S3*E*. (*H*) The UVB-evoked Ca^{2+} signal can be strongly reduced with specific PLC inhibitor, U73122.

of both inhibitors completely eliminated the UVB-induced Ca^{2+} response by 1°MKs (Fig. 5 *A*, *iii*).

Taken together, these findings indicate that UVB-mediated ET1 secretion contributes significantly to the UVB–TRPV4–Ca^{2+} response in vitro. The data further suggest that ET1–ET(R) cosignaling amplifies TRPV4-dependent Ca^{2+} signals. In support of this notion, the UVB–Ca^{2+} response could be recapitulated by omitting UVB exposure and instead cotreating 1°MKs with ET1 and the selective TRPV4 activator 4α-PDD. This specific response was significantly attenuated by ET(R)-A inhibition and greatly diminished by ET(R)-B inhibition (Fig. 5*B*). There were a few slight changes to the UVB response, namely, codependency of both ET(R)s for UVB, and recruitment of ET(R)-B more than -A for 4α-PDD. These minor differences were not surprising, given the pleiotropic effects of UVB. These results provided compelling support for the interdependency of TRPV4 and ET(R) signaling.

Unstimulated 1°MKs produced appreciable levels of ET1, whose secretory behavior was dependent upon TRPV4 and PLC, as shown by use of specific inhibitors and $Trpv4^{-/-}$ 1°MKs (Fig. S4*B*). We therefore tested whether UVB caused ET1 up-regulation in a TRPV4-dependent manner. Given the exquisite wavelength dependence of ET1 expression in 1°MKs (64, 65), we resorted to the UVB light-emitting diode (LED) stimulation device as for Ca^{2+} imaging (Fig. 4*A* and Fig. S3 *A–D*). UVB-exposed 1°MKs showed increased ET1 immunolabeling, which was diminished when cells were preincubated with TRPV4 inhibitors GSK205 and RN1734 (Fig. S4 *C* and *D*). Consistent with its effects on UVB-evoked Ca^{2+} transients and on unstimulated ET1 secretion, PLC inhibitor U73122 also down-regulated ET1. Together, these findings suggest a limited feed-forward mechanism that involves TRPV4-dependent ET1 secretion and increase of ET1 expression in response to UVB, and autocrine/paracrine signaling via ET(R)s. This signaling involves TRPV4-dependent Ca^{2+} influx, which in turn amplifies ET1 signaling in a paracrine/autocrine fashion.

To assess the physiological relevance of our findings in vivo, we exposed mouse paw pads to UVB. An interesting time course of *Edn1* mRNA expression was apparent in paw-pad skin of WT mice, where it peaked after 120 min and relented at 24 h, but remained significantly elevated (Fig. 5*C*). In contrast, there was no regulated expression of *Edn1* in paw-pad skin of $Trpv4^{-/-}$ mice. These findings suggest a more direct regulation of *Edn1* gene expression by TRPV4 in response to UVB. *Edn1* overexpression in epidermal keratinocytes is likely caused by UVB-mediated Ca^{2+} influx at the time of exposure. Protein synthesis and secretion follow, and the process seems to be maintained in a delimited feed-forward mechanism, very likely leading to downstream effector mechanisms that enhance tissue damage and pain. Moreover, ET1 protein was readily detected in control epidermis but reduced in TRPV4-deficient epidermis (Fig. 5*D*). TRPV4 was critical for the facilitatory effect of ET1 on nocifensive behavior. Mechanically induced withdrawal behavior after subepidermal ET1 injection was significantly sensitized in control but not in $Trpv4^{-/-}$ mice, both pan- and conditional null (Fig. 5*E*). For the pan-null mice this is a very interesting finding. For the inducible null mice this finding is highly surprising because it suggests that ET1's proalgesic/algogenic effect is fully dependent on TRPV4 in keratinocytes. Although previous studies had shown that ET1 is sufficient to elicit nocifensive behavior (66, 67), the elimination of ET1's proalgesic/algogenic effect in iKO mice was completely unexpected given that both ET(R)s and TRPV4 are expressed by sensory afferents (63), all of them unaffected in tam-treated iKO mice.

Clinical Relevance of Epidermally Derived TRPV4 in Sunburn. Interestingly, TRPV4 was significantly increased in human epidermis of patients with sunburn and UV overexposure [Fig. 6*A* (acute) and Fig. S5 (chronic)]. Compared with healthy skin, a robust increase was also seen for ET1 immunostaining in acute overexposure (Fig. 6 *A* and *B*). These findings suggest that TRPV4 is likely to be involved in the skin's acute tissue response to overexposure to UVB, one of the various responses of human skin to damaging UV radiation.

In view of the observed impact of epidermal-specific TRPV4 deficiency on mouse nociception in response to UVB, and because of the effects of selective TRPV4 blockers on 1°MK in

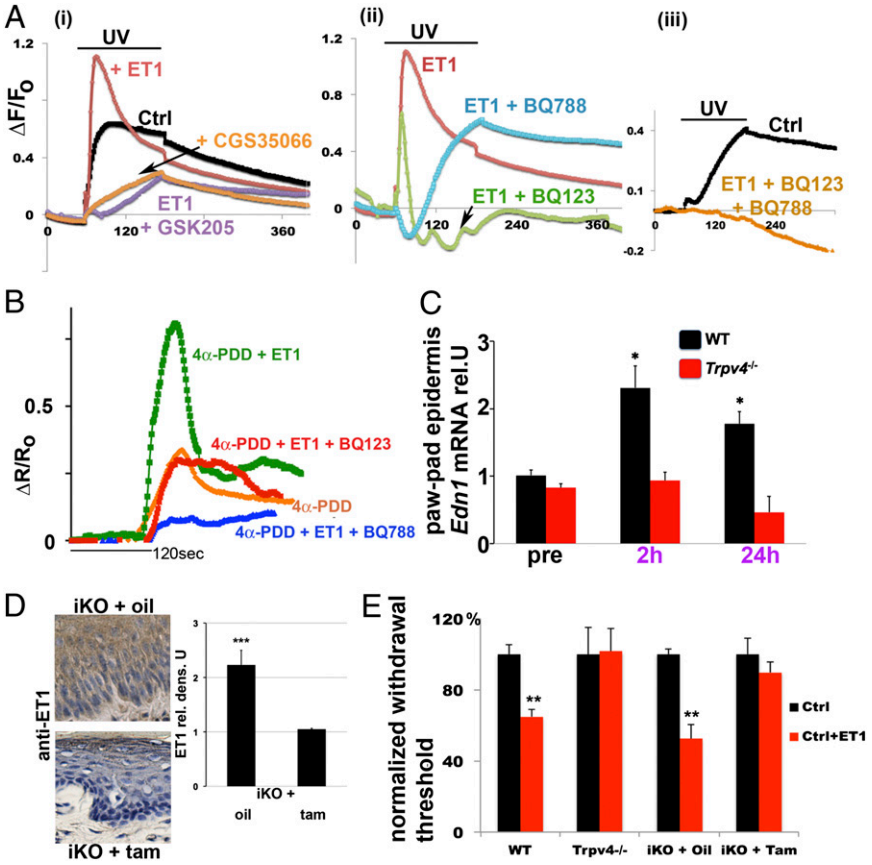

Fig. 5. Central role for keratinocyte TRPV4 in UVB-evoked Ca^{2+} signaling and nocifensive behavior: effects of ET1. (*A*) Effects of ET1 on UVB-evoked Ca^{2+} signaling in 1°MKs. (*i*) Averaged Ca^{2+} transients in 1°MK in response to UVB, their augmentation by coexposure to ET1 peptide, and their significant attenuation by either GSK205, which inhibits TRPV4, or ET-convertase inhibitor CGS35066, which blocks ET1 proteolytic processing. (*ii*) ET-augmented, UVB-induced Ca^{2+} transients as in i, but in this case, their attenuation by selective antagonism of ET(R)-A (using BQ123) and ET(R)-B (using BQ788). (*iii*) The complete elimination of the ET1-augmented Ca^{2+} transients when both subtypes of ET(R) are blocked. (*B*) The 4α-PDD-evoked Ca^{2+} signaling in 1°MKs: ET1-related findings. (*Left*) Ca^{2+} transients (as per fura-2 ratiometric imaging) in response to the selective TRPV4 activator 4α-PDD. A significant increase in the response can be observed by coapplication of ET1, and this is partially dependent on ET(R)-A and completely dependent on ET(R)-B. (*C*) Up-regulation of ET1/*Edn1* in mouse paw in response to UVB. *Edn1* mRNA was determined by qPCR after isolation of total RNA from paw-pad epidermis. Note the early increase, at the 2-h time point, in WT control epidermis, and its complete lack in $Trpv4^{-/-}$, and sustained up-regulation at 24 h, slightly reduced vs. the 2-h time point, again complete lack of up-regulation in $Trpv4^{-/-}$. Quantifications are for $n = 4$ mice per group. **Statistically significant ($P < 0.01$, *t* test). (*D*) Immunohistochemistry reveals a significantly stronger ET1 signal in UVB-exposed skin of oil-treated control vs. tam-treated iKO mice. Note positive labeling of endothelial cells. Quantifications are for $n = 3$ mice per group. ***Statistically significant ($P < 0.001$, *t* test). (*E*) Nocifensive behavior in response to ET1 paw-pad injection depends on epidermal TRPV4. Bar diagram summarizes behavioral findings for $Trpv4^{-/-}$ vs. WT and for oil-treated vs. tam-treated iKO mice. Note that in WT and oil-treated iKO mice paw-pad injection of ET1 leads to significant levels of mechanical allodynia. $Trpv4^{-/-}$ and tam-treated iKO mice fail to respond. Quantifications are for $n = 7$–8 mice per group. **Statistically significant ($P < 0.01$, ANOVA).

vitro, we assessed the translational-medical relevance of our findings. For this purpose, we applied TRPV4 inhibitor GSK205 to WT mouse paw pads topically and subsequently exposed animals to sunburn-inducing doses of UVB (Fig. 7*A*). Whereas vehicle-treated control mice showed normal thermal hypersensitivity, mice treated with 1 mM GSK205 showed an ∼24-h delay in sensitivity, and increasing the dose to 5 mM GSK205 resulted in a sustained attenuation of thermally evoked nocifensive behavior. This treatment also resulted in a significantly reduced sensitivity to von Frey hair mechanical stimulation.

To assess specificity of the external topical treatment, we applied 5 mM GSK205 to $Trpv4^{-/-}$ mice vs. vehicle control mice (Fig. 7*A*). Nocifensive behavior did not show any intergroup differences, yet was significantly different from prestimulation. Thus, topical treatment with 5 mM GSK205 in vivo did not elicit off-target effects on other channels or signaling pathways that might measurably influence withdrawal behavior. Although GSK205-mediated antagonism of macrophage and neural TRPV4 cannot be excluded, the epidermis is the initial target of topically applied drugs, and the effects obtained with 5 mM GSK205 were consistent with those observed in tam-induced iKO mice.

Histopathology of GSK205 topically treated skin showed hallmarks of UVB-mediated sunburn in vehicle-treated paws, strikingly contrasting to GSK205-treated animals (5 mM), whose paws showed virtual elimination of damage (Fig. 7*B*). In view of the TRPV4 dependence of ET/*Edn1* expression in skin, we measured *Edn*1 mRNA abundance in GSK205 vs. vehicle-treated paw-pad skin. We detected an early up-regulation in vehicle-treated mice at the 2-h time point that was still significantly elevated over preexposure animals at 24 h, resembling *Edn1* regulation and time course in untreated WT mice (Fig. 7*C*, compare with Fig. 5*C*). In striking contrast, and in keeping with histopathology, *Edn1* mRNA expression in GSK205 topically treated skin was found unchanged.

To validate these finding, we tested UVB absorption in GSK205-treated paw-pad skin, and whether GSK205 thus functions as a sunscreen. Results were negative, as demonstrated by equal UVB permeation of GSK205- vs. vehicle-treated paw-pad skin, yet valid, as demonstrated by significant decrease of UVB permeation with SPF100 sunscreen (Fig. 7 *D* and *E* and Fig. S6 *A*

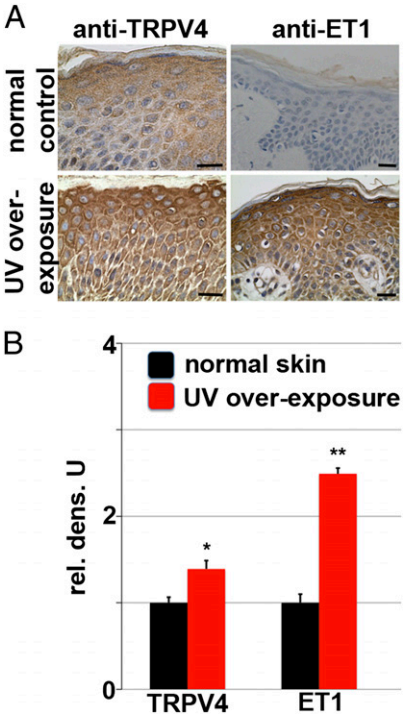

Fig. 6. Epidermal TRPV4 and ET1 are elevated in human skin overexposed to UV. (*A*) Representative micrographs of TRPV4 and ET1 distribution in UV-overexposed epidermis, compared with healthy human skin. Immunostaining for each antigen is increased in the acute tissue response vs. healthy skin. [Scale bars, 50 μm (*Left*), 100 μm (*Right*).] (*B*) Quantitative analysis for immunoreactive TRPV4 and ET1. Findings reveal significantly increased immunolabeling for the two proteins in UV-overexposed epidermis compared with healthy human skin (n = 3 subjects for normal, healthy skin and 3 with UV overexposure).

and *B*). These results corroborate that effects of topically applied GSK205 are caused by TRPV4 antagonism, likely by affecting TRPV4 in epidermal keratinocytes.

Thus, UVB-evoked epidermal signaling was reduced both when TRPV4 was antagonized by topical application of specific small-molecule inhibitors and when *Trpv4* was targeted genetically in iKO mice. This suggests ion channel function of TRPV4 to be the critical factor common to both experimental approaches. Together, these findings render topically applied selective TRPV4 blockers excellent candidates to reduce tissue damage and pain caused by UVB exposure in humans.

Discussion

In this study, we discovered that TRPV4 ion channels in skin keratinocytes are critically involved in the organismal hypersensitivity response that results in tissue injury and pain following acute UVB overexposure, as in sunburn. We found that UVB triggers TRPV4 channel activation, which leads to Ca^{2+} influx into keratinocytes. In turn, this transforms the cells to function in a proalgesic manner.

Specifically, we document TRPV4-dependent early up-regulation of *Edn1* mRNA expression, ET1 secretion, and action on ET(R)s. Although some details of UVB-induced TRPV4 channel activation await further definition, we have identified PLC as a key player, necessary for production of high-activity small-molecule intermediaries such as IP3. Moreover, we find that ET1–ET(R) signaling, which activates PLC, is also essential for Ca^{2+} signaling by epidermal TRPV4, and here, ET1–ET(R) seem to function in an autocrine/paracrine feed-forward loop. Epidermal TRPV4 is absolutely needed for injected ET1 to function in a proalgesic manner.

Beyond rather acute effector responses of the keratinocyte UVB-sentinel system, longer-term adaptive changes elicited by ET1 are relevant. One of these is UVB-induced pigmentation, where endothelins act as a potent inducer of melanocyte differentiation (68–70). Given our finding that epidermal TRPV4 regulates ET1 secretion, TRPV4 becomes poised not only to orchestrate the acute sentinel function of keratinocytes, which induces pain and hypersensitivity, which leads to protective temporary rest and nonuse, but also to provide longer-term protection. Notably, UV dermatitis with subsequent protective pigmentation is a widespread occurrence in the vertebrate kingdom (71), yet pigmentation disorders in humans might also be linked to TRPV4 signaling.

In terms of skin pigmentation, another recent paper reported expression of TRPA1 in human melanocytes and their selective activation by UVA (72), preceded by an earlier report of TRPA1 activation by UVA in heterologous cellular systems (73). The authors demonstrate direct Ca^{2+} signaling in response to UVA that enhances pigmentation in human melanocytes, depending on TRPA1 and opsins. This finding indicates perhaps a molecular spectrum of the skin to match the natural wavelengths that animals encounter so that organismal and skin protection against noxious light/radiation is enhanced. These mechanisms comprise different nonneural cells of the skin. These cells have a TRP ion channel as a central component of the molecular apparatus, and light/radiation-evoked transduction of the channel leads to Ca^{2+} influx. Shorter UVB wavelengths transduce via TRPV4, expressed in keratinocytes, which in the first place leads to tissue injury and pain and secondly to protective hyperpigmentation via the action of ET1 on melanocytes. Longer UVA wavelengths transduce via TRPA1, expressed in melanocytes, which enhances their pigmentation. The role of TRPA1 expression in human keratinocytes in response to UV radiation remains to be determined (74 and see also 75).

Finally, our discovery places TRPV4 as a prime therapeutic target for treatments aimed at alleviating the pain, tissue damage, and skin blistering associated with sunburn. To this end, we have shown that the mechanisms uncovered here in mice are likely to operate in UVB-exposed human skin, and we have demonstrated the effectiveness of topically applying TRPV4 inhibitors (76).

Experimental Procedures

See *SI Experimental Procedures* for more details.

Animals. The *Trpv4* genomic locus was engineered so that loxP sites surrounded exon13, which encodes TM5-6. This mutation was propagated in mice that were crossed to *K14*-CRE-ER^{tam} mice, so that ((*Trpv4*$^{lox/lox}$)*X*(*K14*-CRE-ER^{tam})) mice could be induced by tam administration via oral gavage for five consecutive days at 6 mg/d in 0.3 mL corn oil, at age 2–4 mo of age, plus a one-time booster 2 wk after the last application. Male and female mice were induced equally. Efficiency of targeting was verified by qRT-PCR for *Trpv4* using primers sense 5′-CCTGCTGGTCACCTACATCA and antisense 5′-CTCAGGAACACAGGGAAGGA, with the former primer located in exon 13. All animal experimentation described here was conducted in full compliance with National Institutes of Health and Duke University internal guidelines, and under a valid Institutional Animal Care and Use Committee protocol.

Behavioral Assessment of Withdrawal Thresholds and UVB Stimulation. Behavioral tests were performed to evaluate the decrease in withdrawal thresholds in response to mechanical von Frey hair or thermal stimuli applied to hind paws. Tests were conducted as previously published (37). These withdrawal thresholds were ascertained before and after UV exposure. Mice were exposed 3–5 d after the last application of tam/oil, using a Bio-Rad Gel Doc 2000 UV transilluminator (302 nm) for 5 min with an exposure of 600 mJ/cm^2. This represent 5–10 times the minimal erythema-inducing dose (77–79), in keeping with our rationale of inducing sunburn and studying sunburn-evoked pain.

In Vivo Topical Interventions. ***ET1 injections.*** After determining baseline withdrawal thresholds, each animal received an intraplantar injection of 10 μL 100 nM ET1 plus contralateral vehicle. Thresholds were again evaluated 1 h after injection.

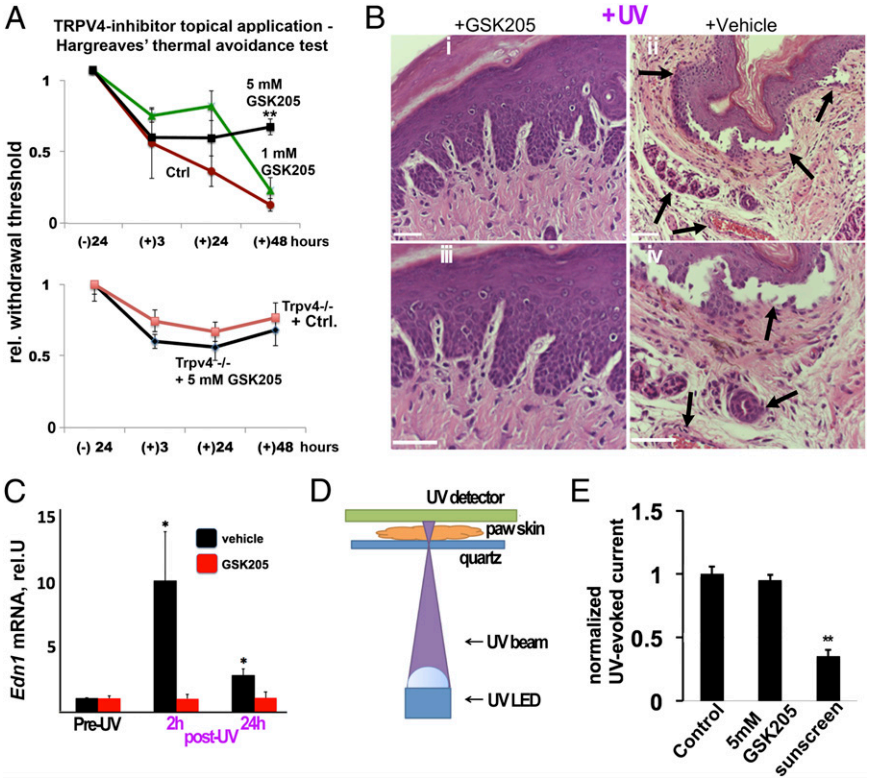

Fig. 7. External topical application of a selective TRPV4 inhibitor attenuates UVB-evoked nocifensive behavior and skin tissue injury. (*A*) UVB-induced nocifensive behavior. Pain behavior is attenuated by topical application of GSK205. (*Upper*) Diagram shows withdrawal thresholds after UVB exposure in response to noxious thermal cues (Hargreaves' test), and their modulation by two doses of topically applied GSK205 (1 mM and 5 mM, applied 60 and 10 min before exposure). The higher dose led to a significant attenuation of thermal allodynia at 48 h post-UVB; $n = 6$ mice per group; $^{**}P < 0.01$ ANOVA. (*Lower*) Diagram shows development of moderate thermal allodynia in *Trpv4*$^{-/-}$ mice, and similar sensitization for vehicle-treated vs. 5 mM GSK205-treated mice, indicating lack of off-target effects of the compound at 5 mM for topical application; $n = 5$ mice per group. (*B*) UVB-evoked sunburn tissue damage is attenuated in mice treated with GSK205. Representative H&E micrographs of paw-pad skin are shown. (Scale bars, 20 μm.) Treatment of UVB-exposed skin with GSK205 improved the skin architecture in mice compared with vehicle-treated mice after 24 h. (i and iii) Representative skin sections of UVB-exposed skin after GSK205 treatment showed markedly reduced cellular infiltrate, less spongiosis, and dermal–epidermal blisters with remaining epidermal thickening. (ii and iv) Vehicle-treated paw pads after UVB exposure were characterized by signs of severe acute sunburn damage such as spongiosis, epidermal hyperkeratosis, disrupted dermal–epidermal border (blister), and a marked cellular infiltrate with dilated blood vessels and dermal edema (arrows). Also note the erythrocyte accumulation in blood vessels, indicating tissue damage and hyperemia. (*C*) Topical treatment with a TRPV4-specific inhibitor attenuates up-regulation of algogenic ET1/*Edn1*. *Edn1* mRNA was determined by qPCR after extraction of total RNA from paw-pad epidermis. In vehicle-treated skin, note increase of *Edn1* expression with robust early up-regulation at the 2-h time point, and sustained moderate elevation up to the 24-h time point. This time course resembles that seen in WT control mice, compared to *Trpv4*$^{-/-}$ mice (Fig. 5*C*). Importantly, topical treatment with 5 mM GSK205 results in complete lack of this regulation; $n = 4$ mice per group, $^{*}P < 0.05$ *t* test. (*D*) GSK205 does not function as sunscreen. The schematic illustrates the experimental setup. (*E*) GSK205 does not function as sunscreen. The bar diagram shows results from $n = 7$–8 mice per group; note absence of a change in UVB permeation with 5 mM GSK205, topically applied as for *A*, vs. vehicle control, yet significantly reduced with sunscreen SPF100.

GSK205 topical treatment. A viscous solution of 68% (vol/vol) EtOH/5% glycerol plus 1 mM or 5 mM GSK205 (none for control) was applied to hind paws by rubbing in 20 μL, applied at time points 1 h and again 10 min before UV exposure.

Formalin-induced nocifensive behavior. Formalin (4%, 10 μL) was injected into the right hind paw, following previous protocols (48). Mice were then videotaped for 50 min and behavior analyzed by blinded observers.

Mouse Tissue Processing for 1-μm Semithin Sections and EM. Samples were processed and subjected to EM as described previously (80).

Mouse and Human Tissue Processing for Immunohistochemistry. Routine procedures were followed as described previously (37, 80, 81). More detail is available in *SI Experimental Procedures*. Human tissue was processed under institutional review board approval (University of California, San Francisco). Informed consent was obtained from all human subjects involved in this research.

Primary Mouse Keratinocyte Cell Culture. Primary mouse keratinocytes were derived from back skin of newborn mice following previously described protocols (80, 81).

Ca^{2+} Imaging of Cultured Keratinocytes. Ca^{2+} imaging of 1°MK was conducted following routine procedures (59, 82). For UVB stimulation, a customized device was built (more detail is given in *SI Experimental Procedures*). The system comprised a printed circuit board for electrical interconnects and mechanical support and a UV LED. Customized provisions at the cellular end included a quartz coverslip as the bottom of the cell culture dish plus a thermal equilibration stage (HW-101; Dagan Corp.), fitted to an Olympus BX61 upright microscope. The UV LED was a III-nitride-based type (UVTOP-295 BL; Sensor Electronic Technology). The operating wavelength was 295 nm (Fig. S3*A*), with a full width at half maximum of 12 nm. The optical power was 500 mW. The focal point was aimed at the plane of the upper surface of the quartz coverslip, which was used to minimize UV absorption along the optical path toward the cells (Fig. S3 *A*–*C*). The optical intensity at the focal point was estimated to be 150 mW/mm^2.

Keratinocyte UV Irradiation Using 295-nm LED and Immunocytochemistry. The 1°MKs were exposed to UVB using the UV optical system (295-nm LED). Twenty-four hours later the cells were fixed and immunolabeled for ET1. Digital images were subjected to morphometry.

Statistical Analysis. Numeric signals or values were averaged for their respective groups and the statistical mean ± SEM (as shown in all diagrams in the figures) were compared between groups by using a fixed-effect one-way ANOVA and post hoc Scheffé test or Student *t* test, at a significance level of $P < 0.05$.

ACKNOWLEDGMENTS. We thank Drs. Sidney Simon and Joerg Grandl (Duke University) for critical comments. Mouse ES cells were generated at the gene-targeting facility of The Rockefeller University (Dr. Chingwen Yang, Director). This work was supported by National Institutes of Health (NIH)/National Institute of Dental and Craniofacial Research Grants DE018549, DE018549S1, and DE018549S2 (to W.B.L.); NIH/National Institute of Arthritis and Musculoskeletal and Skin Diseases (NIAMS) Grants AR059402 and Deutsche Forschugsgemeinschaft [German Research Foundation; DFG] STE 1014/2-2 (to M.S.) and DFG Ce165/1-1 (to F.C.); DFG Ke1672/1-1 (to C.K.); and NIH/NIAMS Grants AR31737 and AR050452 (to E.F.). E.F. is a Howard Hughes Medical Investigator. We also acknowledge NIH/National Institute of Biomedical Imaging and Bioengineering Grant P41 EB015897 for confocal core support (Dr. G. Allan Johnson, Principal Investigator).

1. Fuchs E (2009) Finding one's niche in the skin. *Cell Stem Cell* 4(6):499–502.
2. Roosterman D, Goerge T, Schneider SW, Bunnett NW, Steinhoff M (2006) Neuronal control of skin function: The skin as a neuroimmunoendocrine organ. *Physiol Rev* 86(4):1309–1379.
3. Tominaga M, Caterina MJ (2004) Thermosensation and pain. *J Neurobiol* 61(1):3–12.
4. Patapoutian A (2005) TRP channels and thermosensation. *Chem Senses* 30(Suppl 1): i193–i194.
5. Paus R, Theoharides TC, Arck PC (2006) Neuroimmunoendocrine circuitry of the 'brain-skin connection.'. *Trends Immunol* 27(1):32–39.
6. Joachim RA, et al. (2008) Stress-induced neurogenic inflammation in murine skin skews dendritic cells towards maturation and migration: Key role of intercellular adhesion molecule-1/leukocyte function-associated antigen interactions. *Am J Pathol* 173(5):1379–1388.
7. Lee H, Caterina MJ (2005) TRPV channels as thermosensory receptors in epithelial cells. *Pflugers Arch* 451(1):160–167.
8. Soter NA (1990) Acute effects of ultraviolet radiation on the skin. *Semin Dermatol* 9 (1):11–15.
9. Bishop T, et al. (2007) Characterisation of ultraviolet-B-induced inflammation as a model of hyperalgesia in the rat. *Pain* 131(1-2):70–82.
10. Harrison GI, Young AR, McMahon SB (2004) Ultraviolet radiation-induced inflammation as a model for cutaneous hyperalgesia. *J Invest Dermatol* 122(1): 183–189.
11. Rauschmayr T, Groves RW, Kupper TS (1997) Keratinocyte expression of the type 2 interleukin 1 receptor mediates local and specific inhibition of interleukin 1-mediated inflammation. *Proc Natl Acad Sci USA* 94(11):5814–5819.
12. Svensson CI (2010) Interleukin-6: A local pain trigger? *Arthritis Res Ther* 12(5):145.
13. Edwards RR, et al. (2008) Association of catastrophizing with interleukin-6 responses to acute pain. *Pain* 140(1):135–144.
14. De Jongh RF, et al. (2003) The role of interleukin-6 in nociception and pain. *Anesth Analg* 96(4):1096–1103.
15. Wolf G, Livshits D, Beilin B, Yirmiya R, Shavit Y (2008) Interleukin-1 signaling is required for induction and maintenance of postoperative incisional pain: Genetic and pharmacological studies in mice. *Brain Behav Immun* 22(7):1072–1077.
16. Wolf G, Gabay E, Tal M, Yirmiya R, Shavit Y (2006) Genetic impairment of interleukin-1 signaling attenuates neuropathic pain, autotomy, and spontaneous ectopic neuronal activity, following nerve injury in mice. *Pain* 120(3):315–324.
17. Sacerdote P, Bianchi M, Ricciardi-Castagnoli P, Panerai AE (1992) Tumor necrosis factor alpha and interleukin-1 alpha increase pain thresholds in the rat. *Ann N Y Acad Sci* 650:197–201.
18. Schweizer A, Feige U, Fontana A, Müller K, Dinarello CA (1988) Interleukin-1 enhances pain reflexes. Mediation through increased prostaglandin E2 levels. *Agents Actions* 25(3-4):246–251.
19. Kupper TS, Groves RW (1995) The interleukin-1 axis and cutaneous inflammation. *J Invest Dermatol* 105(1, Suppl):62S–66S.
20. Dawes JM, et al. (2011) CXCL5 mediates UVB irradiation-induced pain. *Sci Transl Med* 3(90):90ra60.
21. Bernard JJ, et al. (2012) Ultraviolet radiation damages self noncoding RNA and is detected by TLR3. *Nat Med* 18(8):1286–1290.
22. Mishra SK, Hoon MA (2010) Ablation of TrpV1 neurons reveals their selective role in thermal pain sensation. *Mol Cell Neurosci* 43(1):157–163.
23. Willis WD, Jr. (2009) The role of TRPV1 receptors in pain evoked by noxious thermal and chemical stimuli. *Exp Brain Res* 196(1):5–11.
24. Lazar J, Gharat L, Khairathkar-Joshi N, Blumberg PM, Szallasi A (2009) Screening TRPV1 antagonists for the treatment of pain: Lessons learned over a decade. *Expert Opinion Drug Discov* 4(2):159–180.
25. Gunthorpe MJ, Chizh BA (2009) Clinical development of TRPV1 antagonists: Targeting a pivotal point in the pain pathway. *Drug Discov Today* 14(1–2):56–67.
26. Patel KN, Liu Q, Meeker S, Undem BJ, Dong X (2011) Pirt, a TRPV1 modulator, is required for histamine-dependent and -independent itch. *PLoS ONE* 6(5):e20559.
27. Schaffler K, et al. (2013) An oral TRPV1 antagonist attenuates laser radiant-heat-evoked potentials and pain ratings from UV(B)-inflamed and normal skin. *Br J Clin Pharmacol* 75(2):404–14.
28. Alenmyr L, Högestätt ED, Zygmunt PM, Greiff L (2009) TRPV1-mediated itch in seasonal allergic rhinitis. *Allergy* 64(5):807–810.
29. Mishra SK, Tisel SM, Orestes P, Bhangoo SK, Hoon MA (2011) TRPV1-lineage neurons are required for thermal sensation. *EMBO J* 30(3):582–593.
30. Imamachi N, et al. (2009) TRPV1-expressing primary afferents generate behavioral responses to pruritogens via multiple mechanisms. *Proc Natl Acad Sci USA* 106(27): 11330–11335.
31. Mishra SK, Hoon MA (2013) The cells and circuitry for itch responses in mice. *Science* 340(6135):968–971.
32. Brierley SM, et al. (2009) The ion channel TRPA1 is required for normal mechanosensation and is modulated by algesic stimuli. *Gastroenterology* 137(6):2084–2095.
33. Cai X (2008) A new tr(i)p to sense pain: TRPA1 channel as a target for novel analgesics. *Expert Rev Neurother* 8(11):1675–1681.
34. Hoffmann T, et al. (2013) TRPA1 and TRPV1 are differentially involved in heat nociception of mice. *Eur J Pain.*, 10.1002/j.1532-2149.2013.00331.
35. McMahon SB, Wood JN (2006) Increasingly irritable and close to tears: TRPA1 in inflammatory pain. *Cell* 124(6):1123–1125.
36. Knowlton WM, McKemy DD (2011) TRPM8: From cold to cancer, peppermint to pain. *Curr Pharm Biotechnol* 12(1):68–77.
37. Liedtke W, Friedman JM (2003) Abnormal osmotic regulation in trpv4-/- mice. *Proc Natl Acad Sci USA* 100(23):13698–13703.
38. Alessandri-Haber N, Joseph E, Dina OA, Liedtke W, Levine JD (2005) TRPV4 mediates pain-related behavior induced by mild hypertonic stimuli in the presence of inflammatory mediator. *Pain* 118(1–2):70–79.
39. O'Neil RG, Heller S (2005) The mechanosensitive nature of TRPV channels. *Pflugers Arch* 451(1):193–203.
40. Nilius B, Vriens J, Prenen J, Droogmans G, Voets T (2004) TRPV4 calcium entry channel: A paradigm for gating diversity. *Am J Physiol Cell Physiol* 286(2):C195–C205.
41. Sipe WE, et al. (2008) Transient receptor potential vanilloid 4 mediates protease activated receptor 2-induced sensitization of colonic afferent nerves and visceral hyperalgesia. *Am J Physiol Gastrointest Liver Physiol* 294(5):G1288–G1298.
42. Alessandri-Haber N, et al. (2004) Transient receptor potential vanilloid 4 is essential in chemotherapy-induced neuropathic pain in the rat. *J Neurosci* 24(18):4444–4452.
43. Chen Y, et al. (2013) Temporomandibular joint pain: A critical role for Trpv4 in the trigeminal ganglion. *Pain* 154(8):1295–1304.
44. Sokabe T, Fukumi-Tominaga T, Yonemura S, Mizuno A, Tominaga M (2010) The TRPV4 channel contributes to intercellular junction formation in keratinocytes. *J Biol Chem* 285(24):18749–18758.
45. Sokabe T, Tominaga M (2010) The TRPV4 cation channel: A molecule linking skin temperature and barrier function. *Commun Integr Biol* 3(6):619–621.
46. Vasioukhin V, Degenstein L, Wise B, Fuchs E (1999) The magical touch: Genome targeting in epidermal stem cells induced by tamoxifen application to mouse skin. *Proc Natl Acad Sci USA* 96(15):8551–8556.
47. Lu CP, et al. (2012) Identification of stem cell populations in sweat glands and ducts reveals roles in homeostasis and wound repair. *Cell* 150(1):136–150.
48. Porro CA, Cavazzuti M (1993) Spatial and temporal aspects of spinal cord and brainstem activation in the formalin pain model. *Prog Neurobiol* 41(5):565–607.
49. Maricich SM, et al. (2009) Merkel cells are essential for light-touch responses. *Science* 324(5934):1580–1582.
50. Maricich SM, Morrison KM, Mathes EL, Brewer BM (2012) Rodents rely on Merkel cells for texture discrimination tasks. *J Neurosci* 32(10):3296–3300.
51. Liedtke W, et al. (2000) Vanilloid receptor-related osmotically activated channel (VR-OAC), a candidate vertebrate osmoreceptor. *Cell* 103(3):525–535.
52. Haeberle H, Bryan LA, Vadakkan TJ, Dickinson ME, Lumpkin EA (2008) Swelling-activated Ca2+ channels trigger Ca2+ signals in Merkel cells. *PLoS ONE* 3(3):e1750.
53. Van Keymeulen A, et al. (2009) Epidermal progenitors give rise to Merkel cells during embryonic development and adult homeostasis. *J Cell Biol* 187(1):91–100.
54. Woo SH, Stumpfova M, Jensen UB, Lumpkin EA, Owens DM (2010) Identification of epidermal progenitors for the Merkel cell lineage. *Development* 137(23): 3965–3971.
55. Chen Y, et al. (2013) Temporomandibular joint pain: A critical role for Trpv4 in the trigeminal ganglion. *Pain* 18(8):1295–1304 10.1016/j.pain.2013.1004.1004.
56. Liu T, van Rooijen N, Tracey DJ (2000) Depletion of macrophages reduces axonal degeneration and hyperalgesia following nerve injury. *Pain* 86(1–2):25–32.
57. Alptekin NO, et al. (2005) Neutrophil elastase levels in periapical exudates of symptomatic and asymptomatic teeth. *J Endod* 31(5):350–353.
58. Vincent F, Duncton MA (2011) TRPV4 agonists and antagonists. *Curr Top Med Chem* 11(17):2216–2226.
59. Li J, et al. (2011) TRPV4-mediated calcium influx into human bronchial epithelia upon exposure to diesel exhaust particles. *Environ Health Perspect* 119(6):784–793.
60. Moqrich A, et al. (2005) Impaired thermosensation in mice lacking TRPV3, a heat and camphor sensor in the skin. *Science* 307(5714):1468–1472.
61. Peier AM, et al. (2002) A heat-sensitive TRP channel expressed in keratinocytes. *Science* 296(5575):2046–2049.
62. Knock GA, et al. (1993) Characterization of endothelin-binding sites in human skin and their regulation in primary Raynaud's phenomenon and systemic sclerosis. *J Invest Dermatol* 101(1):73–78.
63. Khodorova A, Montmayeur JP, Strichartz G (2009) Endothelin receptors and pain. *J Pain* 10(1):4–28.
64. Tsuboi R, et al. (1995) Ultraviolet B irradiation increases endothelin-1 and endothelin receptor expression in cultured human keratinocytes. *FEBS Lett* 371(2):188–190.
65. Ahn GY, et al. (1998) The expression of endothelin-1 and its binding sites in mouse skin increased after ultraviolet B irradiation or local injection of tumor necrosis factor alpha. *J Dermatol* 25(2):78–84.
66. Namer B, et al. (2008) Endothelin 1 activates and sensitizes human C-nociceptors. *Pain* 137(1):41–49.

67. Motta EM, Calixto JB, Rae GA (2006) Mechanical hyperalgesia induced by endothelin-1 in rats is mediated via phospholipase C, protein kinase C, and MAP kinases. *Exp Biol Med (Maywood)* 231(6):1141–1145.
68. Gilchrest BA, Park HY, Eller MS, Yaar M (1996) Mechanisms of ultraviolet light-induced pigmentation. *Photochem Photobiol* 63(1):1–10.
69. Rabbani P, et al. (2011) Coordinated activation of Wnt in epithelial and melanocyte stem cells initiates pigmented hair regeneration. *Cell* 145(6):941–955.
70. Chang CY, et al. (2013) NFIB is a governor of epithelial-melanocyte stem cell behaviour in a shared niche. *Nature* 495(7439):98–102.
71. Martinez-Levasseur LM, et al. (2011) Acute sun damage and photoprotective responses in whales. *Proc Royal Soc B* 278(1711):1581–1586.
72. Bellono NW, Kammel LG, Zimmerman AL, Oancea E (2013) UV light phototransduction activates transient receptor potential A1 ion channels in human melanocytes. *Proc Natl Acad Sci USA* 110(6):2383–2388.
73. Hill K, Schaefer M (2009) Ultraviolet light and photosensitising agents activate TRPA1 via generation of oxidative stress. *Cell Calcium* 45(2):155–164.
74. Atoyan R, Shander D, Botchkareva NV (2009) Non-neuronal expression of transient receptor potential type A1 (TRPA1) in human skin. *J Invest Dermatol* 129(9):2312–2315.
75. Liu B, et al. (2013) TRPA1 controls inflammation and pruritogen responses in allergic contact dermatitis. *FASEB J*, 10.1096/fj.13-229948.
76. Moran MM, McAlexander MA, Bíró T, Szallasi A (2011) Transient receptor potential channels as therapeutic targets. *Nat Rev Drug Discov* 10(8):601–620.
77. Kennedy Crispin M, et al. (2013) Gene profiling of narrowband UVB-induced skin injury defines cellular and molecular innate immune responses. *J Invest Dermatol* 133(3):692–701.
78. Walker SL, Young AR (1997) Sunscreens offer the same UVB protection factors for inflammation and immunosuppression in the mouse. *J Invest Dermatol* 108(2):133–138.
79. Kligman LH, Murphy GF (1996) Ultraviolet B radiation increases hairless mouse mast cells in a dose-dependent manner and alters distribution of UV-induced mast cell growth factor. *Photochem Photobiol* 63(1):123–127.
80. Vasioukhin V, Bauer C, Degenstein L, Wise B, Fuchs E (2001) Hyperproliferation and defects in epithelial polarity upon conditional ablation of alpha-catenin in skin. *Cell* 104(4):605–617.
81. Vasioukhin V, Bowers E, Bauer C, Degenstein L, Fuchs E (2001) Desmoplakin is essential in epidermal sheet formation. *Nat Cell Biol* 3(12):1076–1085.
82. Yeo M, Berglund K, Augustine G, Liedtke W (2009) Novel repression of Kcc2 transcription by REST-RE-1 controls developmental switch in neuronal chloride. *J Neurosci* 29(46):14652–14662.